

# High-modulation depth modulator based on double-layer graphene with a low bias voltage

Zhou Dapeng<sup>1</sup>, Xiao Binggang<sup>1</sup> ✉, Xiao Lihua<sup>2</sup>, Guo Fenglei<sup>1</sup>, Wang Xiumin<sup>1</sup>

<sup>1</sup>College of Information Engineering, China Jiliang University, Hangzhou 310018, People's Republic of China

<sup>2</sup>College of Chemical Engineering, Zhejiang University of Technology, Hangzhou 310014, People's Republic of China

✉ E-mail: bgxiao@cjlu.edu.cn

Published in *Micro & Nano Letters*; Received on 29th August 2018; Revised on 1st December 2018; Accepted on 15th January 2019

An efficient modulation can be obtained by graphene due to its outstanding light-matter interaction, and many kinds of modulators based on graphene have been studied during the last couple of years. However, there still exist unsolved issues in graphene-based modulators, such as how to make a balance between modulation depth and modulation bandwidth. This work proposes a reflective modulator with relatively high-modulation depth and wide working bandwidth. The proposed modulator has a simple five-layered structure of graphene–silica–graphene–silicon–metal. They use an effective method of finite element method to simulate the performance of this modulator, and obtain a modulation depth of 96% with a low bias voltage of  $\sim 4$  V. Furthermore, they calculate the modulation speed by the equivalent circuit method, and obtain the maximum modulation speed of about 25 kHz and a wide broadband of 72 kHz from theoretical analysis. Therefore, this high-performance modulator provides an effective method for terahertz communication devices.

**1. Introduction:** Terahertz (THz) waves covering a frequency range from 0.1 to 10 THz has become a hotspot research in wireless communications due to its many advantages, such as high transmission rate, enhanced band source, strong anti-interference ability and so on [1–3]. Thus communication devices of different kinds which work in THz area have been studied in recent years, such as modulators, absorbers and so on [4, 5].

Graphene is a two-dimensional (2D)-honeycomb-lattice material which has drawn an increase in research because of its excellent properties, such as high-electron mobility, tunable chemical energy and Hall effect at room temperature since it was peeled off from carbon in 2004 [6–9]. There is a great prospect that graphene can improve the performance of communication devices, especially in modulators [10]. Therefore, many kinds of modulators based on graphene in THz have been studied and optimised in recent years. For example, in 2017, Xia *et al.* [11] designed a THz amplitude modulator based on graphene with a metallic square ring resonant structure. The maximum modulation depth could reach 72% with a bias voltage of  $-20$  V according to their simulation. However, they did not discuss the modulation speed and the bandwidth. In 2018, Ji *et al.* [12] proposed two heterostructures ferroelectric superlattices modulators with modulation depths of 48.7 and 78.5%, but the energy consumption was a bit higher under that bias voltage swept from  $-40$  to  $40$  V. We can see that it is difficult to achieve a modulator with high-modulation depth, low bias voltage, wide bandwidth and fast modulation speed at the same time. It is still an unsolved challenge.

In this Letter, we propose a reflective THz wave modulator based on double-layer graphene. The structure of this modulator is mainly composed of five layers in a manner of graphene–silica–graphene–silicon–metal. An external voltage was connected to the contacts on the surface of graphene and the metal film. We use a finite element numerical simulation software to simulate the performance of the proposed modulator by adjusting the bias voltage to change the conductivity of graphene, altering the thickness of silicon and silicon dioxide. As such, we obtain a modulation depth reaching up to 96% with a low insertion loss. Its modulation rate is about 25 kHz, and the 3 dB bandwidth 72 kHz. Our results are competitive with some previous studies [13–18]. This modulator has the advantages like a simple structure, high-modulation depth, low bias voltage, wide operation bandwidth and fast modulation rate.

**2. Design:** The proposed modulator is shown in Fig. 1*a*. We can see that the structure of this modulator is simple which is easy to fabricate in the laboratory. The silicon material is p-type with a thickness of  $460 \mu\text{m}$ , and the relative permittivity of silicon is 11.9 in the THz region. As for the silicon dioxide, we can grow a single layer on the surface of graphene with a thickness of  $150 \pm 10$  nm by the chemical vapour deposition (CVD) method in the laboratory. The size of the proposed device here is  $1 \text{ cm} \times 1 \text{ cm}$ , so the graphene is cut into  $1 \text{ cm}^2$  which equals to the device's dimension. Also we can use the same method to grow graphene on the surface of silicon dioxide. At last, gold electrodes can be plated on the surface of graphene which can help to connect the external bias voltage.

The absorption rate of graphene sheet can be modulated by tuning the conductivity of graphene by some methods, such as the continuous wave (CW) laser method or bias voltage method [15, 19]. Therefore, we consider using the bias voltage to control the absorption of graphene indirectly [17] (as shown in Fig. 1*b*). The operating principle of this modulator can be described as follows: when the gate voltage is biased, the absorption of graphene increased with the increment of gate voltage within a certain range. Due to this sandwich structure, there exist two resonant cavities which are composed by the graphene and multi-layer dielectrics, when the THz signal is being absorbed fully which results '0' code (the THz wave reflection is 0.0425). When the gate voltage is unbiased, the graphene just works as a thin film (means above 2.3% of absorption from the previous study [20]), then a larger amplitude of signal can be detected and this could be translated into the digital signal '1' code (the THz wave reflection reaches 0.9492) [21, 22]. The device can be characterised using a THz imaging and spectroscopy setup based on a Virginia Diode, Inc. multiplier source, capable of providing CW radiation in the 620–700 GHz frequency band and a broadband Schottky diode detector (as shown in Fig. 1*c* which is mentioned in [17]).

**3. Simulation:** Graphene is a 2D material. Its many high-performance properties have been analysed since it was discovered the first time. Those properties of graphene can be described by the surface conductivity which has been fully studied in the past few years [23–25]. In the visible light and infrared areas, the surface conductivity is mainly referred to interband transition; however, the other part of it is the intraband transition which domains THz

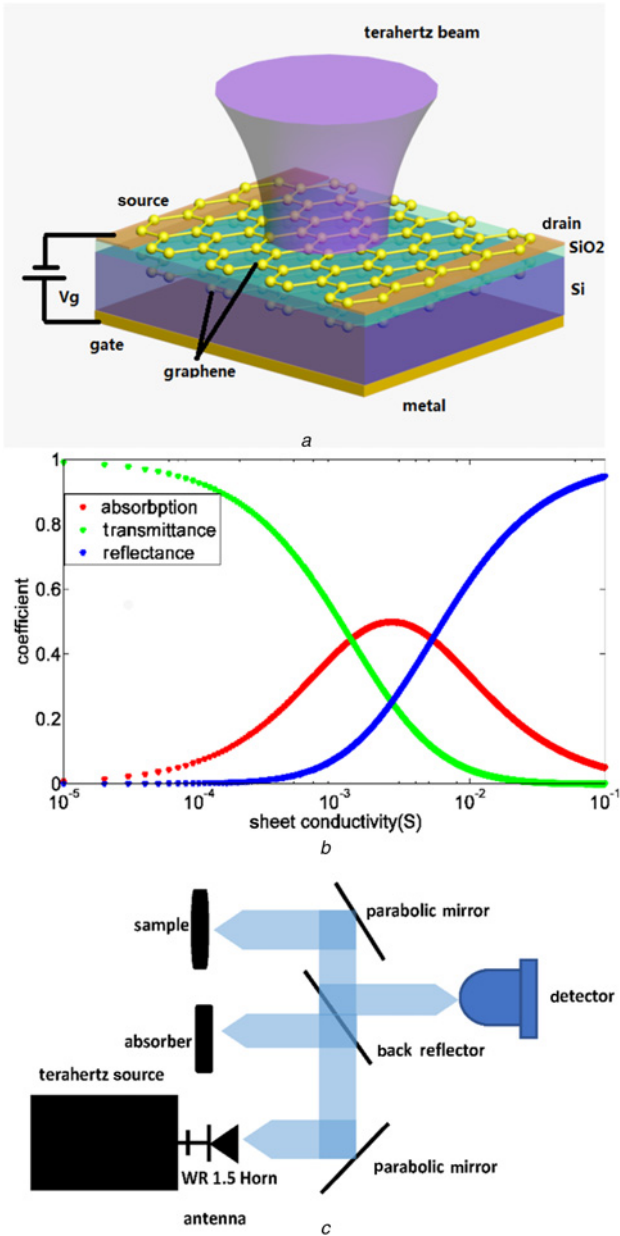


**Fig. 1** The working principle diagram of modulator  
*a* Schematic diagram of the modulator  
*b* Modelled reflectance, transmittance and absorption of a single-layered graphene as a function of its conductivity  
*c* Schematic diagram of the THz imaging and spectroscopy setup [17]

area. In this Letter, the conductivity of graphene is derived from Kubo model [26]

$$\sigma(\omega, \mu_c, \Gamma, T) = \frac{je^2}{\pi\hbar^2(\omega - j2\Gamma)} \left\{ \int_0^\infty \varepsilon \left[ \frac{\partial f_d(\varepsilon)}{\partial \varepsilon} - \frac{\partial f_d(-\varepsilon)}{\partial \varepsilon} \right] d\varepsilon \right\} + \frac{je^2(\omega - j2\Gamma)}{\pi\hbar^2} \left[ \int_0^\infty \frac{f_d(\varepsilon) - f_d(-\varepsilon)}{(\omega - j2\Gamma)^2 - 4(\varepsilon/\hbar)^2} \right] \quad (1)$$

where  $T$  is the temperature,  $\Gamma$  is the scattering rate, and  $\mu_c$  is the chemical potential. The parameter  $\hbar$  stands for normalisation Planck constant, and the function  $f_d(\varepsilon)$  represents the Fermi-Dirac distribution  $\varepsilon$ . When there is only an electric field,

the conversion formula between the chemical potential of graphene and the electric field intensity can be obtained as follows [17]:

$$\frac{\varepsilon_0 \pi \hbar^2 v_F^2}{q_c} E_0 = \int_{\Delta}^{\infty} \varepsilon [n_F(\varepsilon) - n_F(\varepsilon + 2\mu_c)] d\varepsilon \quad (2)$$

where  $v_F$  is Femi velocity,  $n_F(\varepsilon)$  is the carrier concentration. In the specific calculation, we often use the bias voltage to represent different graphene chemical potentials (Fig. 2a). The bias voltage can be calculated according to the following formula [27]:

$$\varepsilon_b E_0 = \varepsilon_r \varepsilon_0 V_g / d \quad (3)$$

where  $\varepsilon_r$  is the relative permittivity of dielectric, and  $d$  is the thickness of the dielectric, and  $V_g$  is the external bias voltage. The relative permittivity of graphene is directly related to graphene conductivity; thus, its value is needed during the simulation of the modulator when using finite element method (FEM) software. We introduce the thickness of graphene, denoted by  $\Delta_d$ , then the relative permittivity can be calculated as [28]

$$\varepsilon = 1 + \frac{i\delta}{\omega \varepsilon_0 \Delta_d} = 1 - \frac{\text{Im}(\delta)}{\omega \varepsilon_0 \Delta_d} + i \frac{\text{Re}(\delta)}{\omega \varepsilon_0 \Delta_d} \quad (4)$$

where  $\delta$  is the conductivity of graphene,  $\omega$  is the angular frequency, and  $\varepsilon_0$  is the impedance of free space.

The reflection and absorption parameters are calculated by a frequency-domain electromagnetic solver, and the whole 3D structure is simulated with mirror symmetry boundary condition. The incident electric field is at normal incidence to the modulator. Hence, the excitation wave and monitoring of the output are the on same side because of the metal film which is on the bottom of the modulator. The THz signal transmits through the graphene layer four times in total. Due to the metal material on the bottom of the graphene, the signal can be fully absorbed by the graphene easily with a low chemical potential. The reflectance and absorption of the modulator simulated by FEM software are shown in Figs. 2b and c. The reflectance attenuates sharply with the increasing of the chemical potential of graphene. However, the absorption increases because of the metal film on the bottom of the modulator [28]. When the chemical potential of graphene is 0.08 eV, the bias voltage can be easily deduced to be about 2 V both from formula (3) and Fig. 2a. The total voltage is double time of the single layer graphene, which means 4 V. Almost 100% of the signal is absorbed by the graphene when the chemical potential of is 0.08 eV (as shown in Fig. 2c), which means when the '0' code signal is modulated. When the bias voltage is zero, the maximum reflectance is about 100%, then the '1' code signal is modulated. The modulation depth can be described as  $MD = (R(0) - R(1)) / R(0)$ , where  $R(0)$  stands for the reflectance when the digital signal is '0', and  $R(1)$  represents the reflectance of digital signal is '1'. The maximum MD is about 96% at the frequency of 0.677 THz. The relationship between modulation depth and frequency is referred to Fig. 2d.

The modulation speed is influenced by the structure of the modulator, and the structure can be described by a simple equivalent circuit because all dielectrics are unpatented which as shown in Fig. 3. The  $R_g$  and  $C_g$  stand for the resistance and capacitance of graphene, the  $C_d$  is the capacitance of dielectric. The modulation speed can be derived from the following formula [18]:

$$f_{\text{speed}} = \frac{1}{2\pi RC} \quad (5)$$

where  $R$  and  $C$  stand for the resistance and capacitance of the modulator, respectively. In this Letter, the  $R = R_g$  according to the

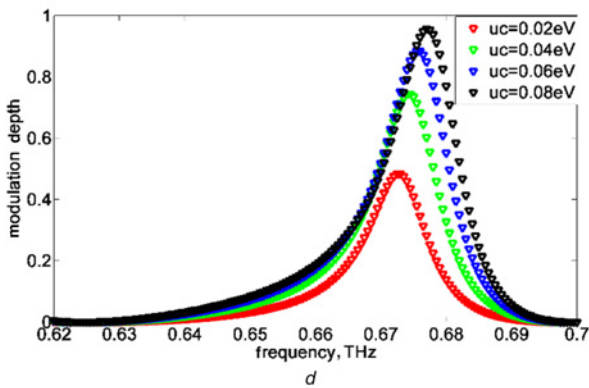
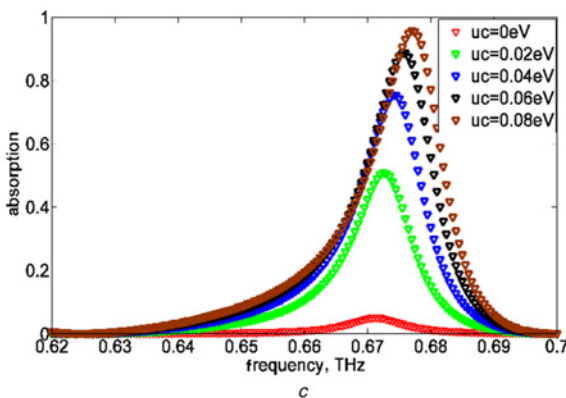
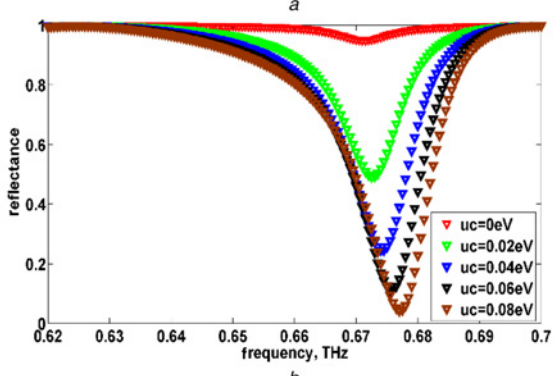
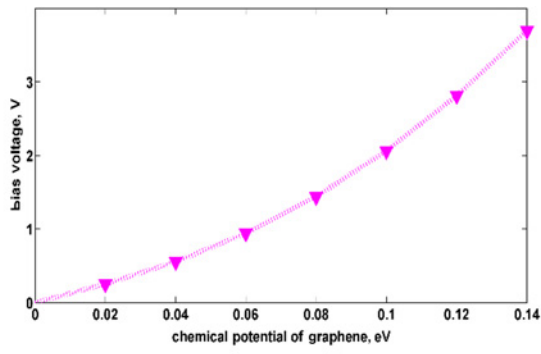


**Fig. 2** Basic performance parameters of simulation  
*a* Chemical potential of graphene versus bias voltage when the thickness of silicon dioxide is 150 nm  
*b* Reflectance versus frequency with different chemical potential  
*c* Absorption versus frequency with different chemical potential  
*d* Modulation depth versus frequency under different chemical potential

previous study [29]. The capacitance of the modulator can be described by the following formula:

$$\frac{1}{C} = \frac{1}{C_g} + \frac{1}{C_d} \quad (6)$$

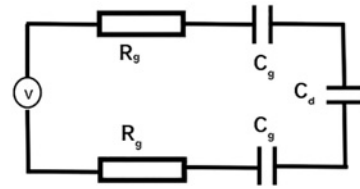


**Fig. 3** Equivalent circuit illustration of the graphene-based modulator. The  $R_g$  and  $C_g$  stand for the resistance and capacitance of graphene, respectively, the  $C_d$  is the capacitance of dielectric

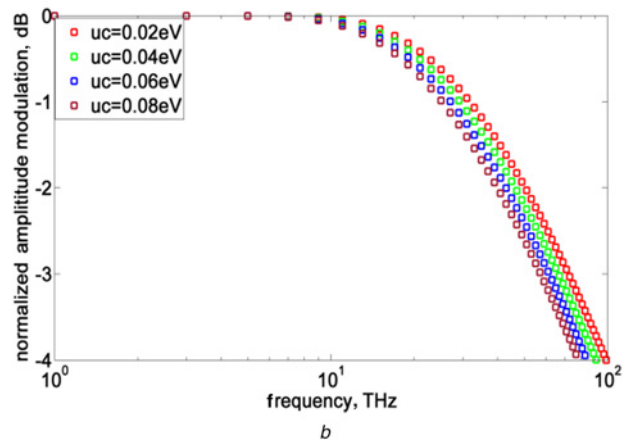
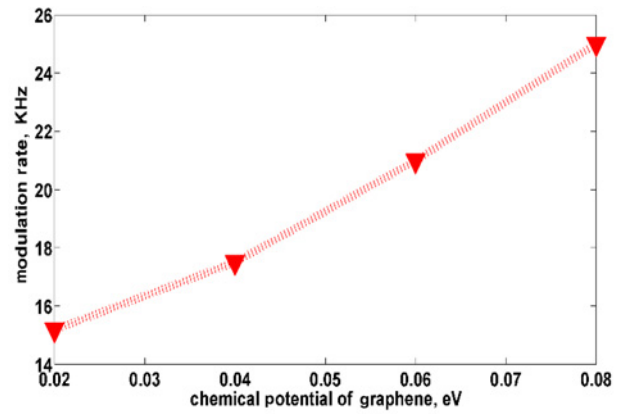


**Fig. 4** Relationship between  
*a* Modulation speed and bias voltage  
*b* Normalised modulation magnitude and the frequency

The capacitance of  $C_g$  can use the following formula [29]:

$$C_g = \frac{2e^2 kT}{\pi(\hbar v_F)^2} \ln \left[ 2 \left( 1 + \cosh \frac{E_F}{kT} \right) \right] \quad (7)$$

where  $e$  is an electronic charge,  $T$  is the room temperature,  $K$  is the Boltzmann constant,  $\hbar$  is the reduced Planck constant, and  $E_F$  is the Fermi level of graphene.  $C_d$  can be calculated by a well-known model of capacitance

$$C_d = \frac{\epsilon_0 \epsilon_r S}{d} \quad (8)$$

where  $\epsilon_0$  is the permittivity of vacuum,  $\epsilon_r$  is the permittivity of dielectric, and  $S$  is the area of graphene. At last, the modulation speed can be found from formulae (5)–(8) and the relationship between

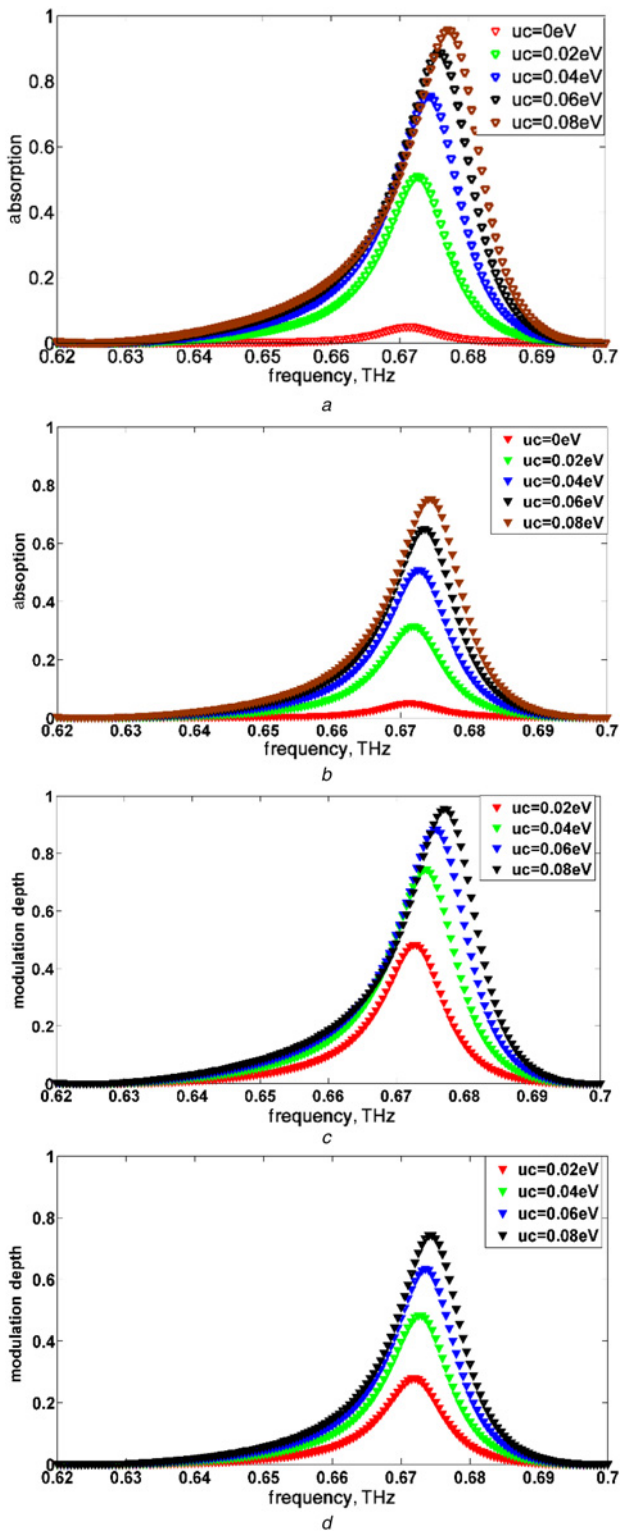


**Fig. 5** Reflectance of modulator at different bias voltages  
 a Single-layer graphene  
 b Single-layer graphene  
 c Double-layer graphene  
 d Double-layer graphene  
 Relationship between modulation depth and frequency at different bias voltages

modulation speed and the bias voltage is shown in Fig. 4a. When the gate voltage is 4 V, the capacitance of this modulator is calculated to be  $2.3 \times 10^{-8}$  F from a silicon dioxide with a thickness of 150 nm, and the resistance of the modulator is found to be about

276  $\Omega$ . Then the modulation speed is 25 kHz, and the 3 dB bandwidth is about 72 kHz which is higher than the similar devices mentioned in [17, 18] (as shown in Fig. 4b).

**4. Discussion:** The p-type silicon is regarded as an ideal material whose relative permittivity is 11.9 in this THz region. It works as a semiconductor which can contact the metal on the bottom of the modulator and the middle graphene that is grown using the method of CVD. The graphene can be grown on the surface of copper by the CVD method in the laboratory, and then transferred to Si/SiO<sub>2</sub> substrate which has been cut to a square with an area of 1 cm<sup>2</sup>. The contacts to the graphene layers can be defined by photolithography and deposited by e-beam evaporation of Au with a Cr adhesion layer. The layers of graphene can make a big difference to the performance of the modulator. When there is a single-layer graphene on the top surface of SiO<sub>2</sub>, the maximum absorption is 74% which is smaller than that with a double-layer graphene (97%) at the same frequency (as shown in Figs. 5a and c). Since the multi-absorption works better when using the double-layer graphene. Thus, the maximum modulation depth (76%) is lower than the double-layer graphene modulator (96%, as shown in Figs. 5b and d), so the performance of double-layer graphene is better than monolayer graphene.

**5. Conclusion:** In conclusion, we have demonstrated a high-performance modulator based on double-layer graphene, of which the maximum modulation depth can reach up to 96% with a wide operation bandwidth of about 72 kHz under a low bias voltage via simulation. Moreover, the modulation depth is greater than some previous studies. It is important that it is easy to fabricate because of its simple shape. The performance of the proposed modulator can further be optimised by tuning the number of graphene layers or the dimension of parameters. Our design provides an effective way to design the THz communication devices.

**6. Acknowledgments:** This work was supported by the 2016 Zhejiang Provincial Natural Science Foundation under grant no. LY16F010010, in part by the 2015 Zhejiang Province Public Welfare of International Cooperation Project under grant no. 2015C34006 and in part by the 2013 National Natural Science Foundation of China under grant no. 61379027.

## 7 References

- [1] Kan T., Isozaki A., Kanda N., *ET AL.*: 'Enantiomeric switching of chiral metamaterial for terahertz polarization modulation employing vertically deformable mems spirals', *Nat. Commun.*, 2015, **6**, (1), p. 8422
- [2] Subkhangulov R.R., Mikhaylovskiy R.V., Zvezdin A.K., *ET AL.*: 'Terahertz modulation of the Faraday rotation by laser pulses via the optical Kerr effect', *Nat. Photonics*, 2016, **10**, (2), pp. 111–114
- [3] Liu M., Yin X., Ulinavila E., *ET AL.*: 'A graphene-based broadband optical modulator', *Nature*, 2011, **474**, (7349), pp. 64–67
- [4] Gomez-Diaz J.S., Moldovan C., Capdevila S., *ET AL.*: 'Self-biased reconfigurable graphene stacks for terahertz plasmonics', *Nat. Commun.*, 2015, **6**, p. 6334
- [5] Kim B.J., Jang H., Lee S.K., *ET AL.*: 'High-performance flexible graphene field effect transistors with ion gel gate dielectrics', *Nano Lett.*, 2010, **10**, (9), pp. 3464–3466
- [6] Wu B., Tuncer H.M., Naeem M., *ET AL.*: 'Experimental demonstration of a transparent graphene millimetre wave absorber with 28% fractional bandwidth at 140 GHz', *Sci. Rep.*, 2014, **4**, (2), p. 4130
- [7] Hasan M., Sensalorodriguez B.: 'Effect of the intra-layer potential distributions and spatial currents on the performance of graphene symFETs', *AIP. Adv.*, 2015, **5**, (9), p. 183
- [8] Lovat G., Hanson G.W., Araneo R., *ET AL.*: 'Semiclassical spatially dispersive intraband conductivity tensor and quantum capacitance of graphene', *Phys. Rev. B*, 2013, **87**, (11), pp. 42–50
- [9] Peng X.L., Hao R., Li E.P.: 'Terahertz modulator based on graphene-embedded waveguide'. *Int. Conf. on Optical Communications and Networks*, China, 2017

- [10] Xiao B., Sun R., Xie Z., *ET AL.*: 'A terahertz modulator based on double-layer graphene', *Optoelectron. Adv. Mater. Rapid Commun.*, 2015, **9**, (5), pp. 692–695
- [11] Xia L., Zhang X., Wei D., *ET AL.*: 'Graphene terahertz amplitude modulation enhanced by square ring resonant structure', *IEEE Photonics J.*, 2018, **10**, (1), p. 5900107
- [12] Ji J., Zhou S., Zhang J., *ET AL.*: 'Electrical terahertz modulator based on photo-excited ferroelectric superlattice', *Sci. Rep.*, 2018, **8**, (1), p. 2682
- [13] Yan R., Sensalerodriguez B., Liu L., *ET AL.*: 'A new class of electrically tunable metamaterial terahertz modulators', *Opt. Express*, 2012, **20**, (27), p. 28664
- [14] Liang G., Hu X., Yu X., *ET AL.*: 'Integrated terahertz graphene modulator with 100% modulation depth', *Acs Photon.*, 2015, **2**, (11), p. 151019111132002
- [15] Wen Q.Y., Tian W., Mao Q., *ET AL.*: 'Graphene based all-optical spatial terahertz modulator', *Sci. Rep.*, 2014, **4**, p. 7409
- [16] Du W., Li E.P., Hao R.: 'Tunability analysis of a graphene-embedded ring modulator', *Photon. Technol. Lett. IEEE*, 2014, **26**, (20), pp. 2008–2011
- [17] Sensale-Rodriguez B., Yan R., Rafique S., *ET AL.*: 'Extraordinary control of terahertz beam reflectance in graphene electro-absorption modulators', *Nano Lett.*, 2012, **12**, (9), pp. 4518–4522
- [18] Sensalerodriguez B., Yan R., Kelly M.M., *ET AL.*: 'Broadband graphene terahertz modulators enabled by intraband transitions', *Nat. Commun.*, 2012, **3**, (1), p. 780
- [19] He X.: 'Tunable terahertz graphene metamaterials', *Carbon*, 2015, **82**, pp. 229–237
- [20] Ying X., Pu Y., Luo Y., *ET AL.*: 'Enhanced universal absorption of graphene in a Salisbury screen', *J. Appl. Phys.*, 2017, **121**, (2), p. 023110
- [21] Sensale-Rodriguez B., Fang T., Yan R., *ET AL.*: 'Unique prospects for graphene-based terahertz modulators', *Appl. Phys. Lett.*, 2011, **99**, (11), p. 113104
- [22] Shi Y.X., Li J.S., Zhang L.: 'Graphene-integrated split-ring resonator terahertz modulator', *Opt. Quantum Electron.*, 2017, **49**, (11), p. 350
- [23] Rozhkov A.V., Sboychakov A.O., Rakhmanov A.L., *ET AL.*: 'Electronic properties of graphene-based bilayer systems', *Phys. Rep.*, 2016, **648**, pp. 1–104
- [24] Wei J., Zhang X., Qiu J., *ET AL.*: 'Thermal kinetics and thermo-mechanical properties of graphene integrated fluoroelastomer', *J. Polymer Sci. B Polymer Phys.*, 2015, **53**, (23), pp. 1691–1700
- [25] Wei W., Qu X.: 'Extraordinary physical properties of functionalized graphene', *Small*, 2012, **8**, (14), pp. 2138–2151
- [26] Hanson G.W.: 'Dyadic Green's functions and guided surface waves for a surface conductivity model of graphene', *J. Appl. Phys.*, 2008, **103**, (6), p. 19912
- [27] Yao Z., Huang Y., Wang Q., *ET AL.*: 'Tunable surface-plasmon-polariton-like modes based on graphene metamaterials in terahertz region', *Comput. Mater. Sci.*, 2016, **117**, pp. 544–548
- [28] Du W., Hao R., Li E.P.: 'The study of few-layer graphene based Mach-Zehnder modulator', *Opt. Commun.*, 2014, **323**, (14), pp. 49–53
- [29] Wu L., Liu H., Li J., *ET AL.*: 'A 130 GHz electro-optic ring modulator with double-layer graphene', *Crystals*, 2017, **7**, (3), p. 65